

PEAK HORIZONTAL ACCELERATION AND VELOCITY FROM STRONG-MOTION RECORDS INCLUDING RECORDS FROM THE 1979 IMPERIAL VALLEY, CALIFORNIA, EARTHQUAKE

BY WILLIAM B. JOYNER AND DAVID M. BOORE

ABSTRACT

We have taken advantage of the recent increase in strong-motion data at close distances to derive new attenuation relations for peak horizontal acceleration and velocity. This new analysis uses a magnitude-independent shape, based on geometrical spreading and anelastic attenuation, for the attenuation curve. An innovation in technique is introduced that decouples the determination of the distance dependence of the data from the magnitude dependence. The resulting equations are

$$\log A = -1.02 + 0.249M - \log r - 0.00255r + 0.26P$$

$$r = (d^2 + 7.3^2)^{1/2} \quad 5.0 \leq M \leq 7.7$$

$$\log V = -0.67 + 0.489M - \log r - 0.00256r + 0.17S + 0.22P$$

$$r = (d^2 + 4.0^2)^{1/2} \quad 5.3 \leq M \leq 7.4$$

where A is peak horizontal acceleration in g , V is peak horizontal velocity in cm/sec, M is moment magnitude, d is the closest distance to the surface projection of the fault rupture in km, S takes on the value of zero at rock sites and one at soil sites, and P is zero for 50 percentile values and one for 84 percentile values.

We considered a magnitude-dependent shape, but we find no basis for it in the data; we have adopted the magnitude-independent shape because it requires fewer parameters.

INTRODUCTION

New data, particularly from the 1979 Coyote Lake and Imperial Valley earthquakes in California, provide a much improved basis for making ground-motion predictions at small distances from the source. In this report we update our earlier efforts (Page *et al.*, 1972; Boore *et al.*, 1978, 1980) and we introduce some improvements in statistical technique that should give better determination of the effects of both magnitude and distance on ground motion.

We examine here the dependence of peak horizontal acceleration and peak horizontal velocity on moment magnitude (M), distance, and recording-site geology. The results for velocity should be considered provisional pending the integration of more records. We do not intend to imply a preference for peak horizontal acceleration or velocity as parameters for describing earthquake ground motion; we are simply recognizing their widespread use.

This work differs in several important ways from our previous work. Improvements in statistical analysis techniques permit us to develop prediction equations with an explicit magnitude dependence. The newly available close-in data permit us to extend the prediction equations to zero distance. In doing this we have modified the measure of distance used in the previous work and adopted a different functional form for the prediction equation.

METHOD

We fit the strong-motion data by multiple linear regression using the equation

$$\log y = \sum_{i=1}^N a_i E_i - \log r + br + cS \quad (1)$$

where

$$E_i = 1 \text{ for earthquake } i$$

$$= 0 \text{ otherwise}$$

$$S = 1 \text{ for soil sites}$$

$$= 0 \text{ for rock sites}$$

$$r = (d^2 + h^2)^{1/2}.$$

y is either peak horizontal acceleration or velocity, N is the number of earthquakes in the data sample, and d is the closest distance from the recording site to the surface projection of the fault rupture. Values for a_i , b , and c are determined by the linear regression for a chosen value of h , and h is determined by a simple search procedure to minimize the sum of squares of the residuals. Once the a_i values are determined, they are used to find, by least squares, a first- or second-order polynomial representing the magnitude dependence.

$$a_i = \alpha + \beta M_i + \gamma M_i^2. \quad (2)$$

The use of dummy variables such as E_i and S to divide the data into classes is a well-known technique in regression analysis (Draper and Smith, 1966; Weisberg, 1980). Similar techniques have been used before for classifying strong-motion data according to site geology (for example, Trifunac, 1976; McGuire, 1978). Extension of the technique by employing the variable E_i has the advantage that it decouples the determination of magnitude dependence from the determination of distance dependence. To see an example of this advantage, note that the data from a single earthquake is typically recorded over a limited range of distance. If the regression analysis were done in terms of magnitude and distance simultaneously, errors in measuring magnitude would affect the distance coefficient obtained from the regression. Another advantage of the approach is that it causes each earthquake to have the same weight in determining magnitude dependence and each recording to have the same weight in determining distance dependence, which intuitively seems appropriate. The method can be considered the analytical equivalent of the graphical method employed by Richter (1935, 1958) in developing the attenuation curve that forms the basis for the local magnitude scale in southern California. The method described here might prove to be useful in the development of local magnitude scales.

The form chosen for the regression is the equivalent of

$$y = \frac{k}{r} e^{-qr}$$

where k is a function of M and q is a constant. This corresponds to simple point-source geometric spreading with constant- Q anelastic attenuation. Strictly speaking, this form would apply only to a harmonic component of the ground motion, not to peak acceleration or peak velocity. Since the coefficients are determined empirically, however, we believe the application to peak parameters is an appropriate approximation.

We realize that the rupture surface is not a point source for recording sites close to the rupture in a large earthquake. The source of the peak motion, however, is not the whole rupture surface but rather some more restricted portion of it. Even if rupture were instantaneous over the whole surface, which would seem unlikely, the whole surface could not contribute to the motion at any one time because of finite propagation velocities.

The parameter h is introduced to allow for the fact that the source of the peak motion values may not be the closest point on the rupture. If the source of the peak motion were directly below the nearest point on the surface projection of the rupture, the value of h would simply represent the depth of that source. In reality the value obtained for h incorporates all the factors that tend to limit or reduce motion near the source, including any tendency for the peak horizontal acceleration to be limited by the finite strength of near-surface materials (Ambraseys, 1974). The value of h also incorporates any factors that tend to enhance the motion near the source, in particular, directivity (Boore and Joyner, 1978).

We use moment magnitude (Hanks and Kanamori, 1979) defined as

$$M = \frac{2}{3} \log M_0 - 10.7 \quad (3)$$

where M_0 is seismic moment in dyne cm. We prefer M to surface-wave magnitude or local magnitude because M corresponds to a well-defined physical property of the source. Furthermore the rate of occurrence of earthquakes with different M can be related directly to the slip rate on faults (Brune, 1968; Anderson, 1979; Molnar, 1979; Herd *et al.*, 1981). It has been argued that local magnitude is preferable for use in predicting ground motion for engineering purposes because local magnitude is based on measurements at frequencies in the range of engineering significance. It is not clear that local magnitude is in fact a better predictor of ground motion in that frequency range, but, even if it were, the use of local magnitude for predicting ground motion in a future earthquake might merely have the effect of transferring the uncertainty from the step of predicting ground motion given the local magnitude to the step of predicting the local magnitude. [We have done an analysis predicting peak horizontal acceleration and velocity in terms of Richter local magnitude (Joyner *et al.*, 1981) similar to the analysis presented here in terms of moment magnitude. The results are comparable.]

The closest distance to the surface projection of the fault rupture is taken as the horizontal component of the station distance rather than the epicentral distance or the distance to the surface projection of the center of the rupture, because the latter two alternatives are clearly inappropriate in such important cases as Parkfield 1966 or Imperial Valley 1979 where recording sites are located close to the rupture but far from the epicenter and rupture center. Ideally one would work with the distance to the point on the rupture that contributes the peak motion, but it would be difficult to determine the location of that point for past earthquakes and in the present state of knowledge impossible for future earthquakes. The use of our

measure of distance in the development of prediction equations is the equivalent of considering the placement of strong-motion instruments and the placement of structures as analogous experiments from the statistical point of view.

In our earlier work (Page *et al.*, 1972; Boore *et al.*, 1978; 1980), we used the shortest distance to the rupture as the measure of distance, whereas here we use the shortest distance to the surface projection of the rupture. The reason for the change is the introduction of the parameter h , which makes allowance, among other things, for the fact that the source of the peak motion may lie at some depth below the surface. If we used the former measure of distance for d , then we would be compensating twice for the effect of depth.

To estimate σ_y , the standard error of a prediction made using the procedures described here, we use the equation

$$\sigma_y = (\sigma_s^2 + \sigma_a^2)^{1/2}$$

where σ_s is the standard deviation of the residuals from the regression described by equation (1) and σ_a is the standard deviation of the residuals from the regression described by equation (2). This is based on two assumptions: first, that the error in determining the attenuation curve in equation (1) is negligible compared to the residual of an individual data point relative to that curve and second, that all of the variability σ_a is due to the stochastic nature of the relationship between a_i and M and none is due to measuring error in a_i or M_i such as might be caused by inadequate sampling. We believe that the first assumption is probably true, and the second, although not strictly true, is close enough to give a satisfactory approximation to σ_y .

DATA

The data set for peak acceleration consists of 182 recordings from 23 earthquakes and for peak velocity 62 recordings from 10 earthquakes. Six of the earthquakes in the peak acceleration data set and four of the earthquakes in the peak velocity data set were recorded at only one station. Such data are given zero weight in the analysis. The data sets are restricted to earthquakes in western North America with M greater than 5.0 and to shallow earthquakes, defined as those for which the fault rupture lies mainly above a depth of 20 km. For peak values we use the larger of the two horizontal components in the directions as originally recorded. Others (e.g., Campbell, 1981) have used the mean of the two components. For his data set Campbell reports that, on the average, the larger value for peak acceleration exceeds the mean by 13 per cent. The small symbols on Figure 1 show the distribution of the peak acceleration data in magnitude and distance; the large symbols indicate data points not included in our data set but compared with our prediction equations in Table 5. Figure 2 shows the distribution of the peak velocity data in magnitude and distance.

Table 1 lists the earthquakes and gives the source of data used in assigning magnitudes and station distances. For earthquakes through 1975 the sources of strong-motion data and geologic site data are given in a previous publication (Boore *et al.*, 1978). Many of the acceleration data for these earthquakes were taken from Volume I of the series "Strong-Motion Earthquake Accelerograms" published under the direction of D. E. Hudson by the Earthquake Engineering Research Laboratory of the California Institute of Technology. Volume I of that series was used for acceleration instead of Volume II because the procedures used in producing Volume

II tended to bias the peak acceleration toward lower values. For more recent earthquakes, sources of strong-motion data include Porter (1978), Porcella (1979), Porcella *et al.* (1979), Brady *et al.* (1980), and Boore and Porcella (1981). In addition, unpublished data were made available by the California Division of Mines and Geology, by J. N. Brune for the stations of the cooperative program of the University of California at San Diego and the Universidad Nacional Autonoma de Mexico, and by Kinometrics Inc. for the Shell Oil Company station at Munday Creek, Alaska. Sources of site descriptions for records obtained since 1975 include the U.S. Geological Survey (1977) and Shannon and Wilson Inc. and Agbabian Associates (1978, 1980a, b). In the case of two stations (290 Wrightwood, California, and 1096 Fort Tejon, California), site classifications made by Boore *et al.* (1978) were changed on

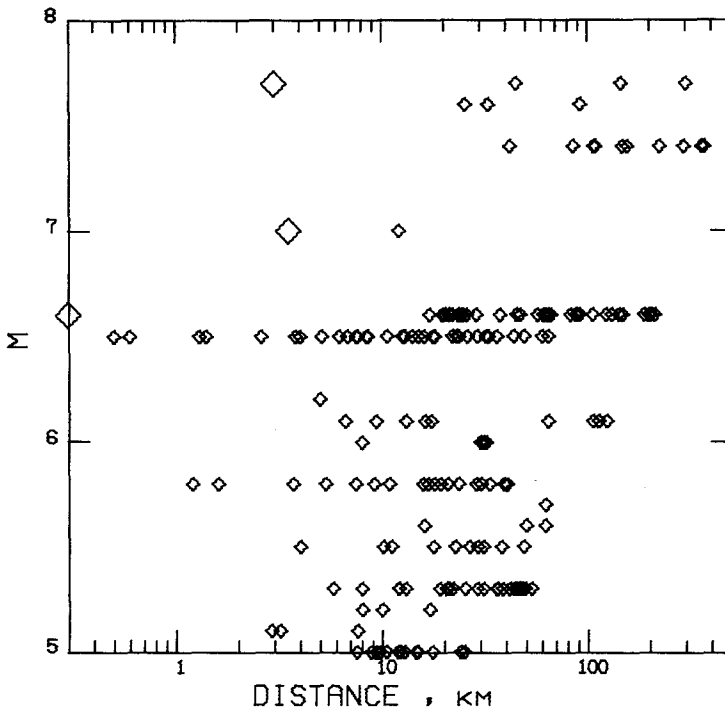


FIG. 1. Distribution in M and d of the data set for peak horizontal acceleration (small symbols). The large symbols show other data points which are compared with the results of the prediction equation in Table 5.

the basis of new information given by Shannon and Wilson Inc. and Agbabian Associates (1978, 1980a, b). The strong-motion data and site classifications are given in Table 2. For some of the recent earthquakes geologic data were not available for all sites. Since only acceleration data were available for those earthquakes and since earlier studies (Boore *et al.*, 1980) had shown that peak acceleration is not correlated with geologic site conditions, we proceeded with the analysis without geologic site data for those earthquakes.

The M values (Table 1) are calculated from seismic moments if moment determinations are available. In cases where they are not available, M is taken to be equal to M_L and the values are enclosed in parentheses in Table 1. The largest such value is 6.2 for the 1972 Managua, Nicaragua, earthquake. This event had an M_S of

6.2 (U.S. Dept. of Commerce, 1973); an M_L of 6.2 was calculated from the strong-motion record at the Esso Refinery (Jennings and Kanamori, 1979).

On the basis of evidence (Boore *et al.*, 1980, Crouse, 1978) suggesting that large structures may bias the ground-motion data recorded at the base of the structure, we excluded from the data set records made at the base of buildings three or more stories in height and on the abutments of dams. We excluded all earthquakes for which the data were in our opinion inadequate for estimating the source distance to an accuracy better than 5 km (see Page *et al.*, 1972, Table 5).

Bias may be introduced into the analysis of strong-motion data by the fact that some operational instruments are not triggered. To avoid this bias we employed the

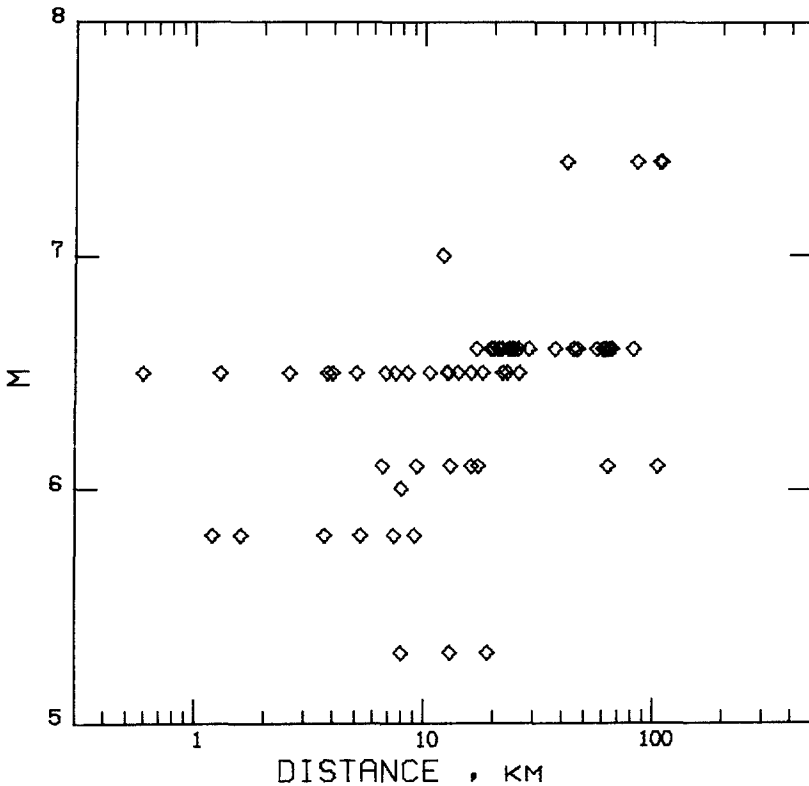


FIG. 2. Distribution in M and d of the data set for peak horizontal velocity.

following procedure: for each earthquake the distance to the nearest operational instrument that did not trigger was determined or in some cases estimated. All data from equal or greater distances for that earthquake were excluded. In contrast to our earlier work the cutoff distance was different for each earthquake. For a few records peak accelerations were reported only as "less than 0.05g." In those cases we noted the smallest distance for such a record and excluded all data recorded at equal or greater distances for that event. There exists a possibility of bias in analyzing peak velocity data because high-amplitude records may have been preferentially chosen for integration. To avoid this bias we noted the distance of the nearest record that had not been integrated, except records for which we knew definitely that the reason they were not integrated had nothing to do with amplitude. We then excluded all velocity data recorded at equal or greater distances for that event.

TABLE 1
SOURCES OF DATA USED IN ASSIGNING MAGNITUDES AND STATION DISTANCES

Earthquake	M	M_L	Date (GMT)			Sources
			Month	Day	Year	
Imperial Valley, California	7.0	6.4	5	19	40	Trifunac and Brune (1970); Trifunac (1972); Richter (1958); Hanks <i>et al.</i> (1975).
Kern County, California	7.4	7.2	7	21	52	Richter (1958); Page <i>et al.</i> (1972); Bolt (1978); Dunbar <i>et al.</i> (1980); Hanks <i>et al.</i> (1975); Boore and Kanamori (unpublished data).
Daly City, California	(5.3)	5.3	3	22	57	Tocher (1959); Cloud (1959).
Parkfield, California	6.1	5.5	6	28	66	McEvelly <i>et al.</i> (1967); Lindh and Boore (1981); Trifunac and Udwardia (1974); Tsai and Aki (1969).
Borrego Mountain, California	6.6	6.7	4	9	68	Kanamori and Jennings (1978); Hamilton (1972); Hanks and Wyss (1972); Swanger and Boore (1978); Hanks <i>et al.</i> (1975).
Santa Rosa, California (2 events)	(5.6) (5.7)	5.6 5.7	10	2	69	Bolt and Miller (1975); Unger and Eaton (1970); J. D. Unger and J. P. Eaton (written communication, 1976).
Lytle Creek, California	5.3	5.4	9	12	70	T. C. Hanks (written communication, 1971); Hanks <i>et al.</i> (1975).
San Fernando, California	6.6	6.4	2	9	71	Allen <i>et al.</i> (1973); Heaton and Helmberger (1979).
Bear Valley, California	5.3	5.1	2	24	72	Bolt and Millter (1975); Ellsworth (1975); Johnson and McEvelly (1974).
Sitka, Alaska	7.7		7	30	72	Page and Gawthrop (1973); Page (oral communication, 1976); Purcaru and Berckhemer (1978).
Managua, Nicaragua	(6.2)	6.2	12	23	72	Jennings and Kanamori (1979); Plafker and Brown (1973); Ward <i>et al.</i> (1973); Knudson and Hansen A. (1973); U.S. Dept. of Commerce (1973).
Point Mugu, California	5.6	6.0	2	21	73	Ellsworth <i>et al.</i> (1973); Boore and Stierman (1976); Stierman and Ellsworth (1976).
Hollister, California	(5.2)	5.2	11	28	74	Cloud and Stifler (1976); W. H. K. Lee (written communication, 1976).
Oroville, California	6.0	5.7	8	1	75	Fogleman <i>et al.</i> (1977); Bufe <i>et al.</i> (1976); Lahr <i>et al.</i> (1976); Langston and Butler (1976); Hart <i>et al.</i> (1977).
Santa Barbara, California	5.1	5.1	8	13	78	Wallace and Helmberger (1979); Lee <i>et al.</i> (1978).
St. Elias, Alaska	7.6		2	28	79	Hasegawa <i>et al.</i> (1980); C. D. Stephens (written communication, 1979); J. Boatwright (oral communication, 1979).

TABLE 1—*Continued*

Earthquake	M	M_L	Date (GMT)			Sources
			Month	Day	Year	
Coyote Lake, California	5.8	5.9	8	6	79	Uhrhammer (1980); Lee <i>et al.</i> (1979).
Imperial Valley, California	6.5	6.6	10	15	79	Kanamori (oral communication, 1981); C. E. Johnson (oral communication, 1979); Boore and Porcella (1981).
Imperial Valley, California aftershock	(5.0)	5.0	10	15	79	C. E. Johnson (oral communication, 1979).
Livermore Valley, California	5.8	5.5	1	24	80	Bolt <i>et al.</i> (1981); R. A. Uhrhammer (oral communication, 1981); J. Boatwright (oral communication, 1980).
Livermore Valley, California	5.5	5.6	1	27	80	Bolt <i>et al.</i> (1981); R. A. Uhrhammer (oral communication, 1981); J. Boatwright (oral communication, 1980); Cockerham <i>et al.</i> (1980).
Horse Canyon, California	(5.3)	5.3	2	25	80	L. K. Hutton (written communication, 1980).

Recording sites were classified into two categories, rock and soil, using the best available information in the same way as done in earlier work (Boore *et al.*, 1978, 1980). Sites described by such terms as "granite," "diorite," "gneiss," "chert," "graywacke," "limestone," "sandstone," or "siltstone" were assigned to the rock category, and sites described by such terms as "alluvium," "sand," "gravel," "clay," "silt," "mud," "fill," or "glacial outwash" were assigned to the soil category, except that if the description indicated soil material less than 4 to 5 m thick overlying rock, the site was classified as a rock site. Resonant frequencies of soil layers as thin as that would generally be greater than 10 Hz and thereby outside the range of frequencies making up the dominant part of the accelerogram.

RESULTS

The a_i values resulting from the regression analysis of peak acceleration data using equation (1) are plotted against M in Figure 3. Earthquakes represented in the data set by only one record are shown in Figure 3 by diamonds and are excluded in the fitting of the polynomial. The coefficient of the second degree term of the polynomial is not significant at the 90 per cent level and the term is omitted.

The effect on the final prediction equations of excluding the points represented by the diamonds in Figure 3 is relatively small. The effect on the 50 percentile values ranges from a 40 per cent increase at magnitude 5.0 to a 10 per cent decrease at magnitude 7.7. The points were excluded in an effort to obtain the best possible estimates of the parameters of the prediction equation. The two lowest points in Figure 3, which represent the two Santa Rosa earthquakes recorded at the same site, are not representative of the earthquakes. In both earthquakes, instruments at eight sites recorded higher peak horizontal acceleration than the record included in the data set even though they were at greater distances (Boore *et al.*, 1978). (These other records were excluded because their distances exceeded the distance of the closest operational instrument that did not trigger.)

PEAK ACCELERATION AND VELOCITY FROM STRONG-MOTION RECORDS 2019

TABLE 2
STRONG-MOTION DATA

Earthquake	Station*	Distance (km)	Peak Horizontal Acceleration (g)	Peak Horizontal Velocity (cm/sec)	Site Condition	
Imperial Valley, 1940 Kern County, 1952	117	12.0	0.359	36.9	soil	
	1083	148.0	0.014		rock	
	1095	42.0	0.196	17.7	soil	
	283	85.0	0.135	19.3	soil	
	135	107.0	0.062	8.9	soil	
	475	109.0	0.054	9.1	soil	
	113	156.0	0.014		soil	
	1008	224.0	0.018		soil	
	1028	293.0	0.010		soil	
	2001	359.0	0.004		soil	
	117	370.0	0.004		soil	
Daly City, 1957	1117	8.0	0.127	4.9	rock	
	1438	16.1	0.411	22.5	rock	
Parkfield, 1966	1083	63.6	0.018	1.1	rock	
	1013	6.6	0.509	78.1	soil	
	1014	9.3	0.467	25.4	soil	
	1015	13.0	0.279	11.8	soil	
	1016	17.3	0.072	8.0	soil	
	1095	105.0	0.012	2.2	soil	
	1011	112.0	0.006		soil	
	1028	123.0	0.003		soil	
	Borrego, Mountain, 1968	270	105.0	0.018		rock
		280	122.0	0.048		rock
116		141.0	0.011		rock	
266		200.0	0.007		rock	
117		45.0	0.142	25.8	soil	
113		130.0	0.031		soil	
112		147.0	0.006		soil	
130		187.0	0.010		soil	
475		197.0	0.010		soil	
269		203.0	0.006		soil	
135	211.0	0.013		soil		
Santa Rosa, 1969 first event	1093	62.0	0.005		soil	
Santa Rosa, 1969 second event	1093	62.0	0.003		soil	
Lytle Creek, 1970	111	19.0	0.086	5.6	rock	
	116	21.0	0.179		rock	
	290	13.0	0.205	9.6	soil	
	112	22.0	0.073		soil	
	113	29.0	0.045		soil	
San Fernando, 1971	128	17.0	0.374	14.6	rock	
	126	19.6	0.200	8.6	rock	
	127	20.2	0.147	4.8	rock	
	141	21.1	0.188	20.5	rock	
	266	21.9	0.204	11.6	rock	
	110	24.2	0.335	27.8	rock	
	1027	66.0	0.057	2.8	rock	
	111	87.0	0.021		rock	
	125	23.4	0.152	18.0	soil	
	135	24.6	0.217	21.1	soil	
475	25.7	0.114	14.3	soil		

TABLE 2—Continued

Earthquake	Station*	Distance (km)	Peak		Site Condition
			Horizontal Acceleration (g)	Horizontal Velocity (cm/sec)	
	262	28.6	0.150	14.2	soil
	269	37.4	0.148	5.4	soil
	1052	46.7	0.112	8.5	soil
	411	56.9	0.043	5.0	soil
	290	60.7	0.057	3.8	soil
	130	61.4	0.030	10.4	soil
	272	62.0	0.027	7.3	soil
	1096	64.0	0.028	1.4	soil
	1102	82.0	0.034	2.5	soil
	112	88.0	0.030		soil
	113	91.0	0.039		soil
Bear Valley, 1972	1028	31.0	0.030		soil
Sitka, 1972	2714	45.0	0.110		rock
	2708	145.0	0.010		rock
	2715	300.0	0.010		soil
Managua, 1972	3501	5.0	0.390		soil
Point Mugu, 1973	655	50.0	0.031		rock
	272	16.0	0.130		soil
Hollister, 1974	1032	17.0	0.011		rock
	1377	8.0	0.120		soil
	1028	10.0	0.170		soil
	1250	10.0	0.140		soil
Oroville, 1975	1051	8.0	0.110	5.0	rock
	1293	32.0	0.040		rock
	1291	30.0	0.070		soil
	1292	31.0	0.080		soil
Santa Barbara, 1978	283	2.9	0.210		
	885	3.2	0.390		
	Goleta substation†	7.6	0.280		
St. Elias, 1979	2734	25.4	0.160		
	Munday Creek‡	32.9	0.064		
	2728	92.2	0.090		
Coyote Lake, 1979	1413	1.2	0.420	43.8	rock
	1445	1.6	0.230	20.5	rock
	1408	9.1	0.130	10.3	rock
	1411	3.7	0.260	32.2	soil
	1410	5.3	0.270	29.4	soil
	1409	7.4	0.260	31.9	soil
	1377	17.9	0.110		soil
	1492	19.2	0.120		soil
	1251	23.4	0.038		soil
	1422	30.0	0.044		soil
	1376	38.9	0.046		soil
Imperial Valley, 1979	Cerro Prieto§	23.5	0.170		rock
	286	26.0	0.210	9.0	rock
	Meloland Overpass¶	0.5	0.320		soil
	5028	0.6	0.520	110.0	soil
	942	1.3	0.720	110.0	soil
	Aeropuerto§	1.4	0.320		soil
	5054	2.6	0.810	44.0	soil
	958	3.8	0.640	53.0	soil
	952	4.0	0.560	87.0	soil
	5165	5.1	0.510	68.0	soil
	117	6.2	0.400		soil

PEAK ACCELERATION AND VELOCITY FROM STRONG-MOTION RECORDS 2021

TABLE 2—Continued

Earthquake	Station*	Distance (km)	Peak Horizontal Acceleration (g)	Peak Horizontal Velocity (cm/sec)	Site Condition
	955	6.8	0.610	78.0	soil
	5055	7.5	0.260	48.0	soil
	Imperial Co. Center¶	7.6	0.240		soil
	Mexicali SAHOP§	8.4	0.460		soil
	5060	8.5	0.220	37.0	soil
	412	8.5	0.230	44.0	soil
	5053	10.6	0.280	19.0	soil
	5058	12.6	0.380	39.0	soil
	5057	12.7	0.270	46.0	soil
	Cucapah§	12.9	0.310		soil
	5051	14.0	0.200	17.0	soil
	Westmoreland¶	15.0	0.110		soil
	5115	16.0	0.430	31.0	soil
	Chihuahua§	17.7	0.270		soil
	931	18.0	0.150	19.0	soil
	5056	22.0	0.150	15.0	soil
	5059	22.0	0.150	15.0	soil
	5061	23.0	0.130	15.0	soil
	Compuertas§	23.2	0.190		soil
	5062	29.0	0.130		soil
	5052	32.0	0.066		soil
	Delta§	32.7	0.350		soil
	724	36.0	0.100		soil
	Victoria§	43.5	0.160		soil
	5066	49.0	0.140		soil
	5050	60.0	0.049		soil
	2316	64.0	0.034		soil
Imperial Valley, 1979 after-shock	5055	7.5	0.264		
	942	8.8	0.263		
	5028	8.9	0.230		
	5165	9.4	0.147		
	952	9.7	0.286		
	958	9.7	0.157		
	955	10.5	0.237		
	117	10.5	0.133		
	412	12.0	0.055		
	5053	12.2	0.097		
	5054	12.8	0.129		
	5058	14.6	0.192		
	5057	14.9	0.147		
	5115	17.6	0.154		
	5056	23.9	0.060		
	5060	25.0	0.057		
Livermore Valley, 1980 24 January	1030	10.8	0.120		
	1418	15.7	0.154		
	1383	16.7	0.052		
	1308	20.8	0.045		
	1298	28.5	0.086		
	1299	33.1	0.056		
	1219	40.3	0.065		
Livermore Valley, 1980 27 January	Fagundes Ranch¶	4.0	0.259		
	Morgan Terrace Park¶	10.1	0.267		
	1030	11.1	0.071		

TABLE 2—Continued

Earthquake	Station*	Distance (km)	Peak Horizontal Acceleration (g)	Peak Horizontal Velocity (cm/sec)	Site Condition
Horse Canyon, 1980	1418	17.7	0.275		
	1383	22.5	0.058		
	Antioch Contra Loma¶	26.5	0.026		
	1299	29.0	0.039		
	1308	30.9	0.112		
	1219	37.8	0.065		
	1456	48.3	0.026		
	5045	5.8	0.123		
	5044	12.0	0.133		
	5160	12.1	0.073		
	5043	20.5	0.097		
	5047	20.5	0.096		
	C168	25.3	0.230		
	5068	35.9	0.082		
	C118	36.1	0.110		
	5042	36.3	0.110		
	5067	38.5	0.094		
	5049	41.4	0.040		
	C204	43.6	0.050		
	5070	44.4	0.022		
C266	46.1	0.070			
C203	47.1	0.080			
5069	47.7	0.033			
5073	49.2	0.017			
5072	53.1	0.022			

* Station numbers preceded by the letter *C* are those assigned by the California Division of Mines and Geology. Other numbers are those assigned by the U.S. Geological Survey (1977; the stations not necessarily being USGS stations).

† Station operated by the Southern California Edison Company.

‡ Station operated by the Shell Oil Company.

§ Station operated by the Universidad Nacional Autonoma de Mexico and the University of California at San Diego.

¶ Station operated by the California Division of Mines and Geology.

Combining the results of the analyses using equations (1) and (2), we obtain the following prediction equation for peak horizontal acceleration

$$\log A = -1.02 + 0.249M - \log r - 0.00255r + 0.26P$$

$$r = (d^2 + 7.3^2)^{1/2} \quad 5.0 \leq M \leq 7.7 \quad (4)$$

where d is defined as in equation (1) and P equals zero for 50 per cent probability that the prediction will exceed the real value and one for 84 per cent probability. The value of P is based on the assumption that the prediction errors are normally distributed, and one could obtain the values of P for other percentiles from a table of the normal distribution function. Because of the limited number of data points, however, the assumption of normality cannot be tested for the tail of the distribution and values of P greater than one should be used with caution. For a few of the recent earthquakes, geologic site data are not available at all sites (Table 2). A preliminary analysis using only the earthquakes for which site data are available

indicated that the soil term is not statistically significant for peak acceleration—a conclusion reached in earlier work (Boore *et al.*, 1980)—and it is therefore not included. Equation (4) is illustrated in Figure 4 for the 50 and 84 percentiles. It is of interest to note that the magnitude coefficient is the same, to two decimal places, as that given by Donovan (1973).

The coefficient of P in equation (4) represents σ_y , the standard error of an individual prediction, and is determined from a value of 0.22 for σ_s , the standard deviation of the residuals from the regression described by equation (1) and a value of 0.13 for σ_a , the standard deviation of the residuals from the regression described by equation (2). The value of 0.26 obtained for σ_y compares well with the value 0.27

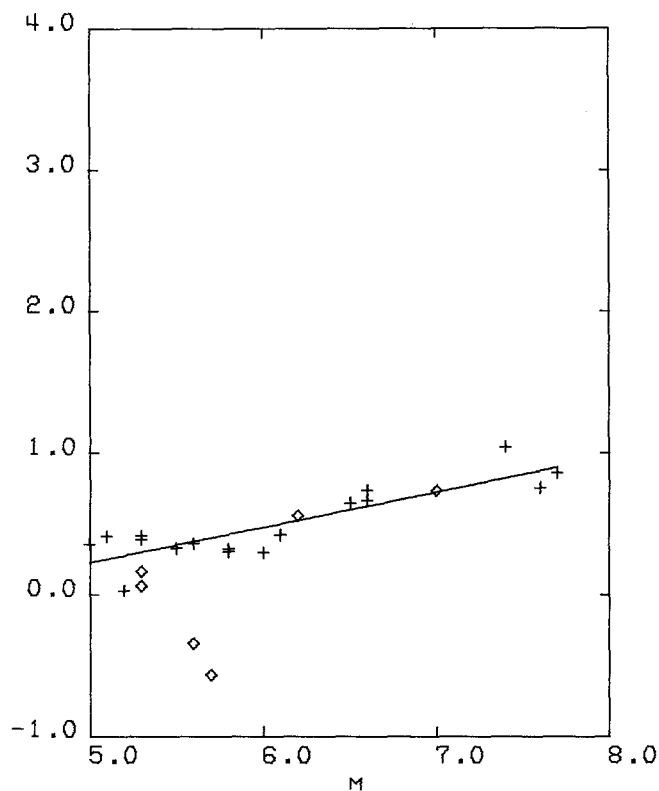


FIG. 3. Values of a_i for peak horizontal acceleration from the regression analysis of equation (1) plotted against moment magnitude. Diamond symbols are earthquakes represented by only one acceleration value; those events were not used in determining the straight line.

obtained by McGuire (1978) using a data set specially constructed to avoid bias in the estimate of residuals caused by multiple records from a single event or by multiple records from the same site of different events.

Residuals of the data with respect to equation (4) are plotted against distance in Figure 5 with different symbols for three magnitude classes. No obvious differences in trend are apparent among the three different magnitude classes, giving no support to the idea that the shape of the attenuation curves depends upon magnitude. Within 10 km the standard deviation appears to be less than the overall average; whether this is the result of the relatively few recordings from a small number of earthquakes or is a general phenomenon awaits further data.

To test further the concept of a magnitude-dependent shape for the attenuation curves, we repeated the analysis of the acceleration data using a magnitude-dependent value of h given by

$$h = h_1 \exp(h_2[M - 6.0]) \quad (5)$$

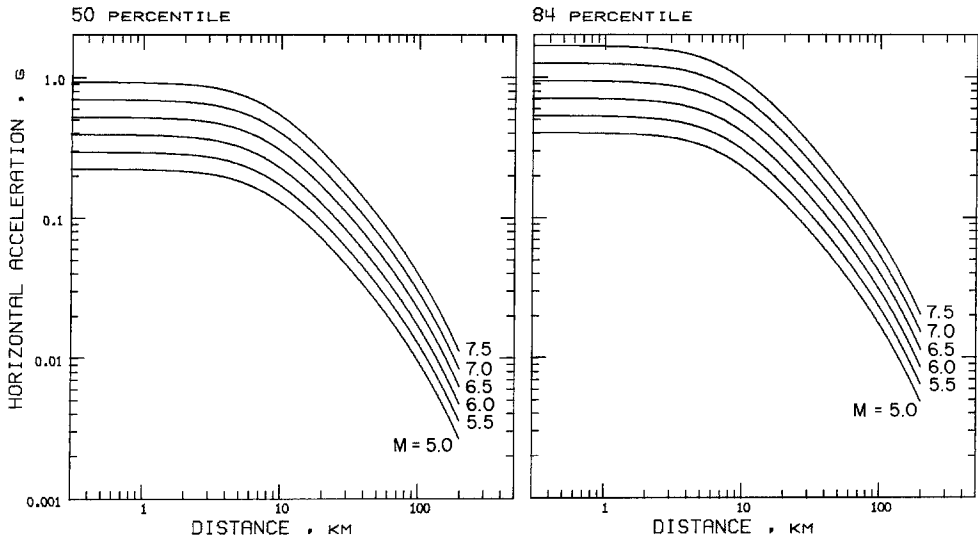


FIG. 4. Predicted values of peak horizontal acceleration for 50 and 84 percentiles as functions of distance and moment magnitude.

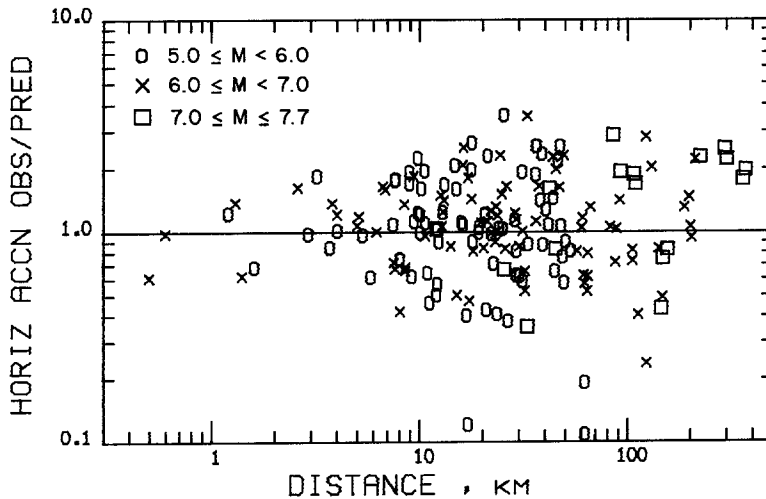


FIG. 5. Residuals of peak horizontal acceleration with respect to equation (4) plotted against distance.

where h_1 and h_2 are determined by minimizing the sum of squares of the residuals. The expression was written in terms of $[M - 6.0]$ rather than simply M in order to reduce the correlation between h_1 and h_2 . We tested the significance of the reduction in variance achieved by going to the magnitude-dependent h , using an approximate

method described by Draper and Smith (1966) for multiple nonlinear regression problems. The reduction in variance is not significant. The distribution of the data set in distance, however, is such that this test is not definitive. The value of h has a large effect on the residuals only for values of d less than about 10 km. Since d is greater than 10 km for most of the data set, changes in h bring relatively small changes in the total variance. A more sensitive test is provided by examining the residuals from equation (4) as a function of magnitude for stations with d less than or equal to 10 km (Figure 6). If there is support in the data for a magnitude-dependent h , it should show as a magnitude dependence in these residuals. A least-squares straight line through the points in Figure 6 has a slope of -0.075 , and the standard deviation of the slope is 0.045. A glance at the plot, however, shows that even this marginal relationship depends on a single earthquake, an aftershock of the 1979 Imperial Valley earthquake, which contributes all of the points plotted at $M = 5.0$. If that earthquake is removed, the least-squares straight line through the

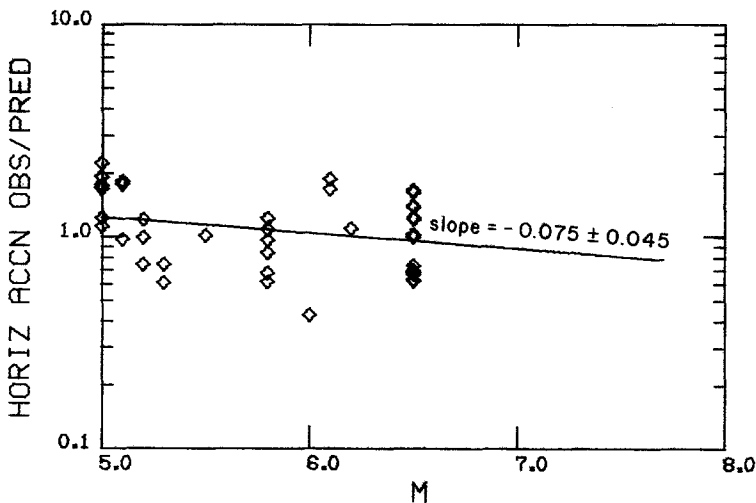


FIG. 6. Residuals of peak horizontal acceleration with respect to equation (4) plotted against M for stations with d less than or equal to 10.0 km.

remaining points has a slope whose value is less than its standard deviation. From this we conclude that the data do not support a magnitude-dependent h . A theoretical argument based on a stochastic source model predicts a slightly magnitude-dependent shape equivalent to choosing $h_2 = 0.12$ in equation (5). The argument is detailed in the Appendix. The resulting prediction equation gives a value of the 50 percentile peak acceleration, for $M = 7.7$ and $d = 0$ only 16 per cent less than that of equation (4). Even if we accepted the model without reservation, we would be disinclined to change the prediction equations for a difference so small. Lacking an adequate basis in the data or in theory for choosing between a magnitude-independent and magnitude-dependent shape for the attenuation curve, we have adopted the magnitude-independent shape because it requires fewer parameters.

In order to demonstrate the sensitivity of the prediction equations to the presence of particular earthquakes in the data set, we recomputed the prediction equations repeatedly, each time excluding a different one (or in some cases two) of the earthquakes. This process was carried out for all of the earthquakes that contribute

TABLE 3
THE EFFECTS OF REMOVING INDIVIDUAL EARTHQUAKES FROM THE DATA SET FOR PEAK HORIZONTAL ACCELERATION

Data Set	Constant Term α	Magnitude Coefficient β	h (km)	Distance Coefficient b	50 Percentile Peak Horizontal Acceleration (g)	
					$M = 6.5$ $d = 0.0$	$M = 7.7$ $d = 0.0$
All earthquakes	-1.02	0.249	7.3	-0.00255	0.52	1.04
San Fernando earthquake omitted	-0.97	0.240	7.3	-0.00241	0.51	0.99
Parkfield earthquake omitted	-0.87	0.223	8.0	-0.00210	0.46	0.85
Kern Co. earthquake omitted	-0.91	0.232	7.6	-0.00294	0.50	0.94
Coyote Lake earthquake omitted	-0.97	0.244	7.8	-0.00257	0.51	0.99
1979 Imperial Valley main shock and after-shock omitted	-1.21	0.275	5.6	-0.00255	0.65	1.40
Borrego Mountain earthquake omitted	-0.97	0.240	7.3	-0.00247	0.51	0.99
Livermore Valley earthquakes omitted	-0.99	0.246	7.3	-0.00257	0.53	1.05
Horse Canyon earthquake omitted	-1.11	0.262	6.7	-0.00254	0.56	1.16

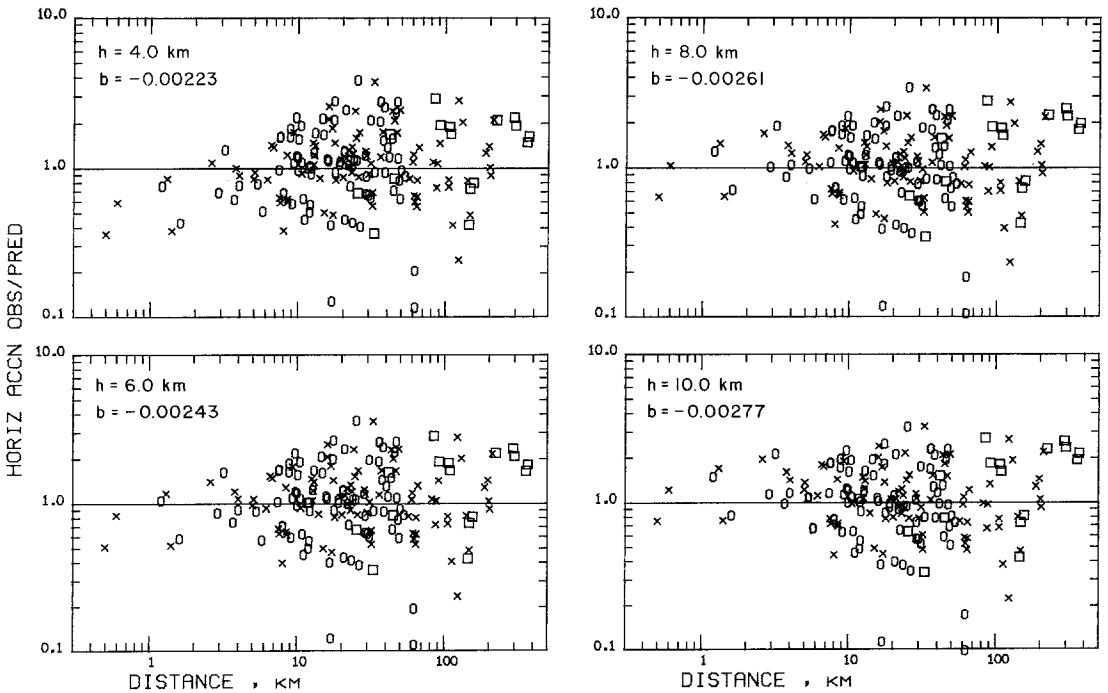


FIG. 7. Residuals of peak acceleration with respect to prediction equations developed using the indicated values of h . Symbols defined as in Figure 5.

a significant fraction of the data set. The results are given in Table 3, which shows the parameters of the prediction equations and the predicted 50 percentile values of peak acceleration at $d = 0$ for $M = 6.5$ and 7.7 .

In order to show the effect of h on the residuals, prediction equations were developed for four different values of h bracketing the value determined by least squares. Residuals against these equations are shown in Figure 7. The value of the distance coefficient b determined by least squares is also shown for each value of h , illustrating the coupling between these two parameters.

The a_i values resulting from the regression of peak velocity data using equation (1) are plotted against M in Figure 8. As with peak acceleration, earthquakes

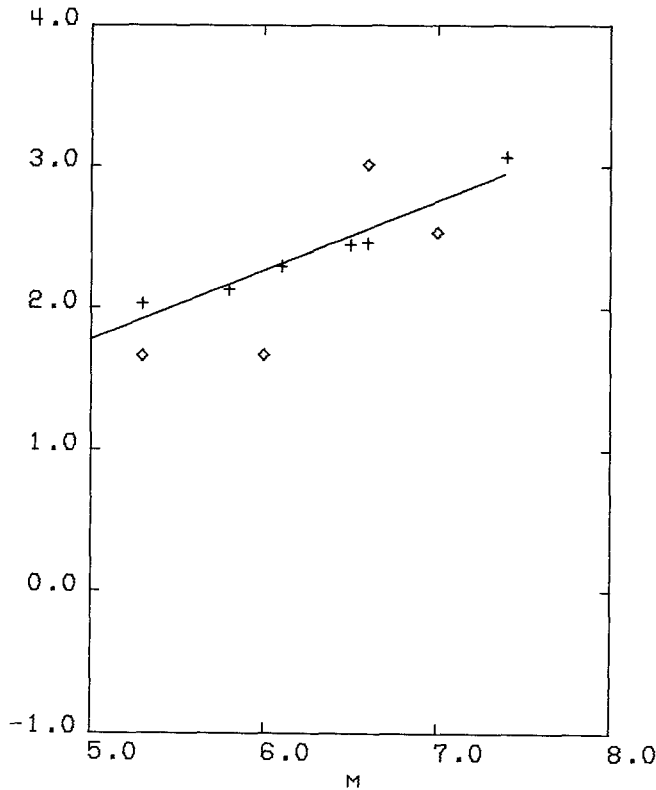


FIG. 8. Values of a_i for peak horizontal velocity from the regression analysis of equation (1) plotted against moment magnitude. Diamond symbols are earthquakes represented by only one velocity value; those events were not used in determining the straight line.

represented in the data set by only one record are shown by diamonds and are excluded in fitting the straight line. It is apparent that the exclusion of these events has a relatively small effect in determining the line but a rather large effect on the standard deviation of points about the line. The coefficient of the second-degree term of the polynomial fitted to the pluses in Figure 8 is statistically significant and leads to a curve concave upward. In view of the small number of points, we have suppressed the second-degree term. The prediction equation for peak horizontal velocity is

$$\log V = -0.67 + 0.489M - \log r - 0.00256r + 0.17S + 0.22P$$

$$r = (d^2 + 4.0^2)^{1/2} \quad 5.3 \leq M \leq 7.4 \quad (6)$$

where d and S are as defined in equation (1) and P is as defined in equation (4). Equation (6) is illustrated in Figure 9.

The soil term in equation (6) is statistically significant at the 98 per cent level in contrast to the case of peak acceleration where it is not significant. Similar results have been reported by Duke *et al.* (1972), Trifunac (1976), and Boore *et al.* (1978, 1980). It seems likely that some sort of amplification mechanisms are operating on the longer periods that are dominant on velocity records and that, for the shorter periods dominant on the acceleration records, these mechanisms are counterbalanced by anelastic attenuation. It is important to note that the determination of the soil effect is dominated by data from southern California where the thickness of low- Q material near the surface is typically large. Net amplification of peak acceleration at soil sites may occur for some other distributions of Q .

The coefficient P in equation (6) is σ_v , the standard error of an individual prediction, and it reflects a value of 0.20 for σ_a , the standard deviation of the

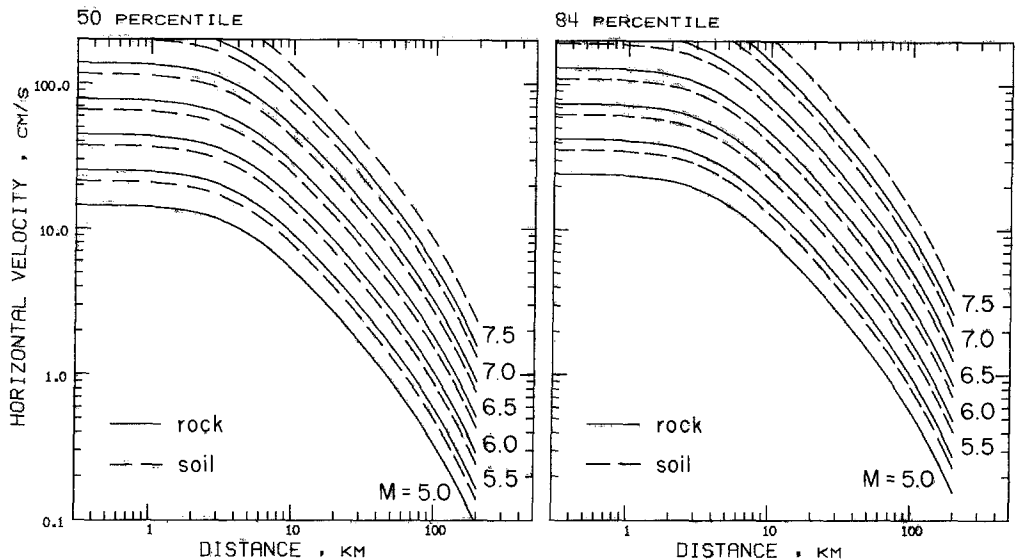


FIG. 9. Predicted values of peak horizontal velocity for 50 and 84 percentile as functions of distance, moment magnitude, and geologic site conditions.

residuals of the regression of equation (1), and a value of 0.10 for σ_a , the standard deviation of the residuals of the regression of equation (2). As with peak acceleration, the value of 0.22 for σ_v compares reasonably well with McGuire's (1978) value of 0.28.

Residuals of the peak velocity data with respect to equation (6) are plotted against distance in Figure 10 for the three different magnitude classes. As with peak acceleration, there are no differences in trend among the different magnitude classes that would support a magnitude-dependent shape for the attenuation curves. As with peak acceleration, we further test the idea of a magnitude-dependent shape by plotting the residuals from equation (6) as a function of magnitude for stations with d less than or equal to 10.0 km (Figure 11). The slope of the least-squares straight line through the points is smaller than its standard error.

The sensitivity of the prediction equations to particular earthquakes in the data set was examined by repeating the computations, each time excluding a different one of the earthquakes. The results are given in Table 4.

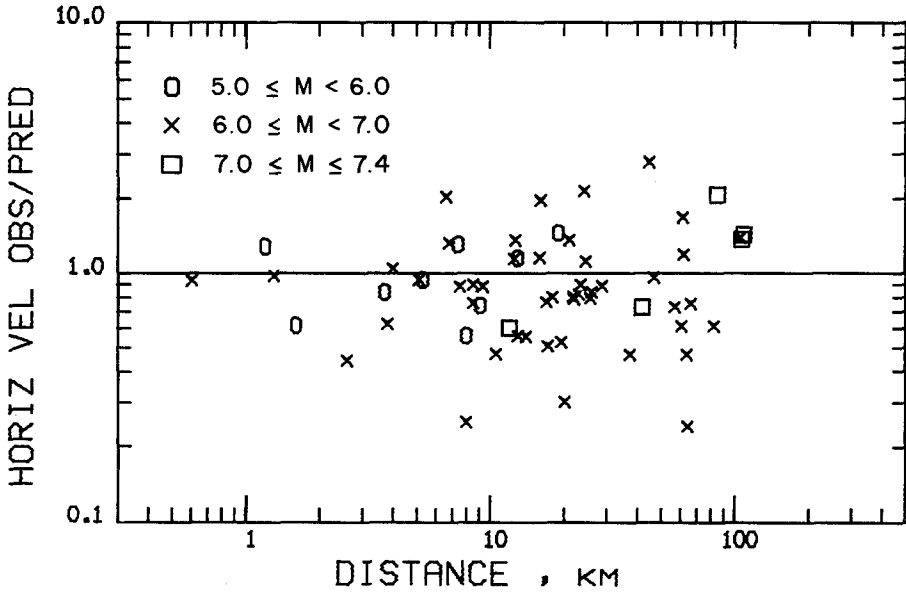


FIG. 10. Residuals of peak horizontal velocity with respect to equation (6) plotted against distance.

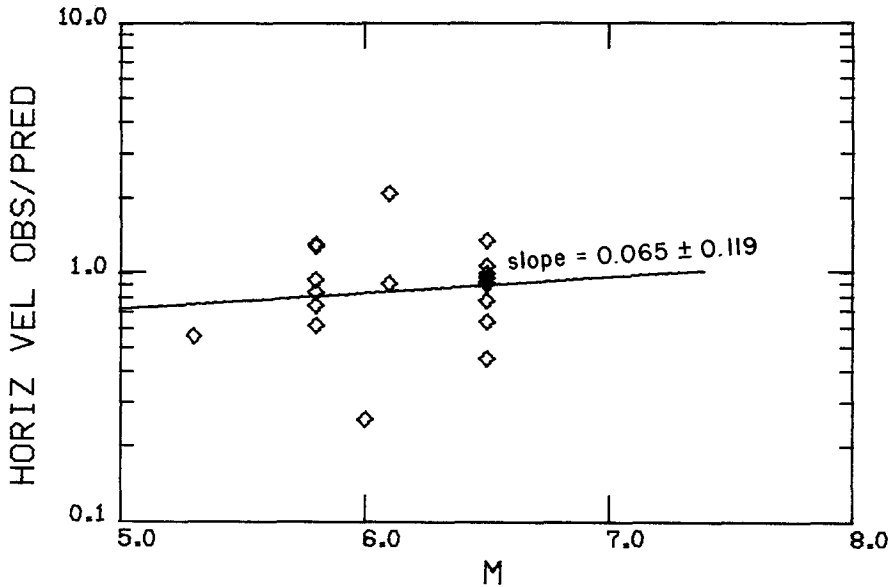


FIG. 11. Residuals of peak horizontal velocity with respect to equation (6) plotted against M for stations with d less than or equal to 10.0 km.

In Figure 12 are shown the residuals of peak horizontal velocity for four different values of h bracketing the value determined by least squares. Also shown is the value of the distance coefficient b determined by least squares for each value of h .

DISCUSSION

The prediction equations are presented in terms of moment magnitude for convenience and for ease of comparison with other studies. Seismic moment, however, is the fundamental parameter, and we believe it desirable to repeat the prediction equations, expressed directly in terms of moment.

$$\log A = -3.68 + 0.166 \log M_0 - \log r - 0.00255r + 0.26P$$

$$r = (d^2 + 7.3^2)^{1/2} \quad 23.5 \leq \log M_0 \leq 27.6$$

$$\log V = -5.90 + 0.326 \log M_0 - \log r - 0.00256r + 0.17S + 0.22P$$

$$r = (d^2 + 4.0^2)^{1/2} \quad 24.0 \leq \log M_0 \leq 27.2$$

(Moment in dyne cm)

The prediction equations are constrained by data at soil sites over the whole distance range of interest for M less than or equal to 6.5, the value for the Imperial Valley earthquake. The data set contains no recordings at rock sites with d less than 8 km for earthquakes with M greater than 6.0, and caution is indicated in applying the equations to rock sites at shorter distances for earthquakes of larger magnitudes. Some indication of the applicability of the equations under those conditions can be obtained by comparing the predicted and observed values, given in Table 5, for the Pacoima Dam record of the San Fernando earthquake ($d = 0.0$

TABLE 4

THE EFFECTS OF REMOVING INDIVIDUAL EARTHQUAKES FROM THE DATA SET FOR PEAK HORIZONTAL VELOCITY

Data Set	Constant Term α	Magnitude Coefficient β	h (km)	Distance Coefficient b	Site Effect Coefficient c	50 Percentile Peak Horizontal Velocity (cm/sec)	
						$M = 6.5$ $d = 0.0$ $S = 1$	$M = 7.4$ $d = 0.0$ $S = 1$
All earthquakes	-0.67	0.489	4.0	-0.00256	0.17	116	321
San Fernando earthquake omitted	-0.55	0.465	3.8	-0.00150	0.19	119	313
Parkfield earthquake omitted	-0.62	0.483	4.3	-0.00253	0.17	111	302
Kern Co. earthquake omitted	0.12	0.359	4.2	-0.00338	0.17	97	204
Coyote Lake earthquake omitted	-0.60	0.481	3.9	-0.00248	0.15	119	323
1979 Imperial Valley earthquake omitted	-0.74	0.501	3.4	-0.00250	0.17	140	396

km, $M = 6.6$). The Pacoima Dam site is a rock site, but the record was excluded from the data set used in the regression analysis because it was recorded on a dam abutment. The observed values are higher than the predicted values for both acceleration and velocity, but the difference is less than the standard error of prediction (σ_y) for velocity and also for acceleration if the observed acceleration is corrected for topographic amplification (Boore, 1973).

For distances less than 40 km from earthquakes with M greater than 6.6, the prediction equations are not constrained by data, and the results should be treated with caution. An indication of the applicability of the equation for acceleration in that range of magnitude and distance can be had by comparing predicted and observed values, given in Table 5, for the Tabas, Iran, and Gazli, USSR, records. These records were not included in the data set because they did not originate in western North America.

We do not propose use of the prediction equations beyond the magnitude limits of the data set, 7.7 for peak acceleration and 7.4 for peak velocity, but we do note that Figures 3 and 8 show no tendency for either peak acceleration or peak velocity

to saturate with magnitude. We do not believe that a valid basis now exists for specifying the behavior of peak acceleration and velocity at magnitudes beyond the limits of our data set. Although it might be argued that peak acceleration and peak velocity should saturate for the same reason that the body-wave magnitude scale

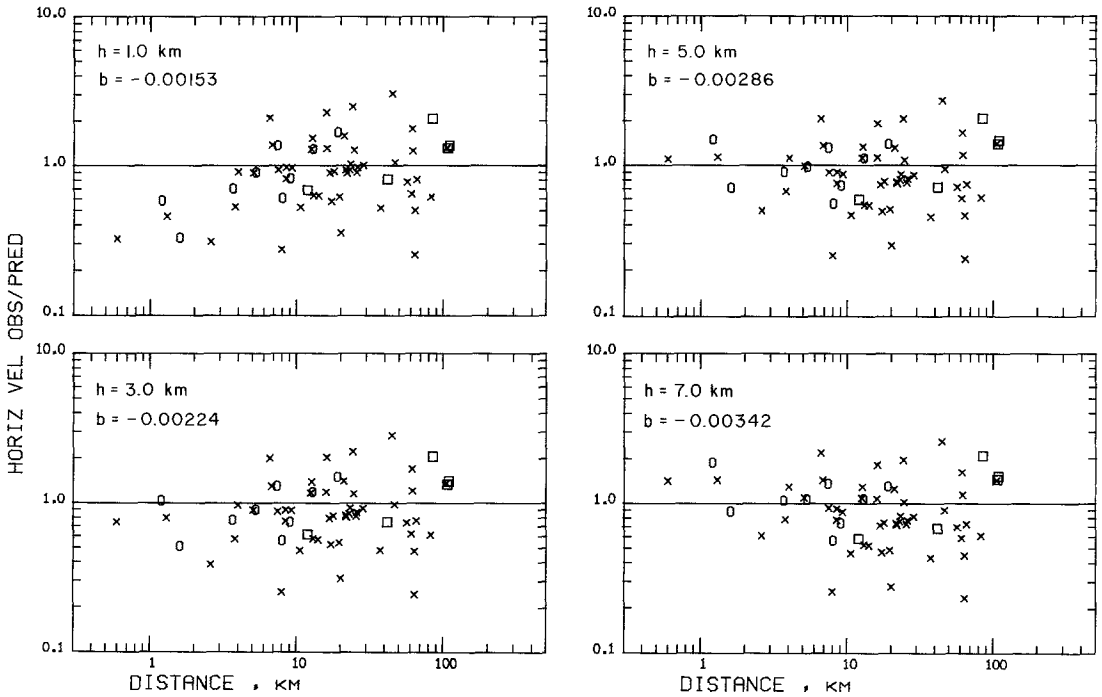


FIG. 12. Residuals of peak velocity with respect to prediction equations developed using the indicated values of h . Symbols defined as in Figure 10.

TABLE 5
COMPARISON OF VALUES GIVEN BY THE PREDICTION EQUATION WITH VALUES FOR SELECTED STRONG-MOTION RECORDS NOT IN THE DATA SET

Record	M	d (km)	Observed Value	Predicted Value
Pacoima Dam Abutment, San Fernando Earthquake (Boore <i>et al.</i> , 1978)	6.6	0.0		
Peak horizontal acceleration			1.25 <i>g</i>	0.55 <i>g</i>
Peak horizontal acceleration corrected for effect of topography (Boore, 1973)			0.73 <i>g</i>	
Peak horizontal velocity			113 cm/sec	88 cm/sec
Karabyr site, Gazli, USSR, earthquake (Campbell, 1981)	7.0	3.5	0.81 <i>g</i>	0.62 <i>g</i>
Tabas, Iran (Campbell, 1981)	7.7	3.0	0.80 <i>g</i>	0.95 <i>g</i>

saturates, we are not aware of any careful analysis supporting this argument. We consider the question open. The recent demonstration by Scholz (1981) that mean slip in large earthquakes correlates linearly with fault length will certainly have an important bearing on these questions.

The prediction equations predict peak velocities greater than 200 cm/sec for M greater than or equal to 7.0 at close distances. No values that high have ever been observed but we know of no physical reason why they could not occur. At soil sites in an earthquake of M greater than 6.5, the finite strength of the soil might limit the peak acceleration to values smaller than those given by the prediction equations, but determining what that limit would be would require adequate *in situ* determination of the dynamic soil properties.

On the basis of fewer available data, Trifunac (1976) made estimates comparable to ours for the peak velocity at small distances from earthquakes of magnitude 7.0 and above. Kanamori (1978) gave an estimate of 200 cm/sec for the peak velocity at 10 km from an earthquake like Kern County ($M = 7.4$), a value somewhat greater than ours (Figure 6). Both Trifunac (1976) and Kanamori (1978) employed the attenuation curve used for local magnitude determinations in southern California. That curve is only weakly constrained by data at short distances. Recent data, especially from the 1979 Imperial Valley earthquake, enable us to develop more closely constrained curves for both acceleration and velocity.

The attenuation relationships developed by Campbell (1981; Campbell *et al.*, 1980) for peak horizontal acceleration are compared in Figure 13 with our results. His definition of peak horizontal acceleration differed from ours in that he used the mean of the two components rather than the larger of the two. To compensate for this we have raised his curves in Figure 13 by 13 per cent, a value determined by him. He selected magnitudes to be consistent with a moment-magnitude scale, essentially M_L for $M \leq 6$ and M_S for $M > 6$. His measure of distance was "the shortest distance from the site to the rupture zone," whereas our measure is the shortest distance to the surface projection of the rupture. This will make no difference for the large magnitude events, which typically break the surface, but the difference may be significant for the smaller events in which the rupture zone may be at significant depth below the surface. His curve for magnitude 5.5 is cut off at 5 km in Figure 13 because at smaller distances the difference in definition of distance invalidates the comparison. He included only data with distances less than 50 km, which severely limits the number of data points included from higher magnitude events.

The differences shown on Figure 13 are small compared to statistical prediction uncertainty. The most conspicuous difference is the change in shape with magnitude shown by his curves, which may be in part due to the different definition of distance. All things considered, we view the relative agreement between the two sets of curves as more significant than the differences. It suggests that the results of both studies are insensitive to rather large variations in method and assumptions.

It is of some interest to consider the physical interpretation of the parameters in the attenuation relationship. If the values agree with what we would expect from other considerations, we gain more confidence that the model, though oversimplified, is appropriate. The value determined for the attenuation coefficient in the relationship for peak acceleration corresponds to a Q of 700 for an assumed frequency of 4 Hz and 350 for a frequency of 2 Hz. The latter value is probably the more appropriate one to consider because the distant records with frequencies closer to 2 Hz than to 4 Hz dominate in the determination of the attenuation coefficient. The value of the attenuation coefficient in the relationship for peak velocity corresponds to a Q of 180 for an assumed frequency of 1 Hz. These Q values lie in the range generally considered appropriate on the basis of other data and increase our confidence in the model. The smaller value for velocity than for acceleration is consistent with the

frequency dependence of Q described by Aki (1980), but in view of the oversimplified character of the model, we do not propose this as evidence for a frequency-dependent Q .

The values of 7.3 and 4.0 km for h in the relationships for peak acceleration and peak velocity seem reasonable in the sense that they lie in the range of $\frac{1}{4}$ to $\frac{1}{2}$ of the thickness of the seismogenic zone in California, where most of the data were recorded. Why the value is less for velocity than for acceleration is not clear. It might be argued that the larger value of h for peak acceleration represents a limitation in acceleration near the source by the limited strength of the near-surface materials. If that were the case, however, one would expect the attenuation curve for earthquakes of magnitude less than 6 to differ in shape from that of earthquakes greater than 6. Figures 5 and 6 show no evidence of this. Another possibility relates

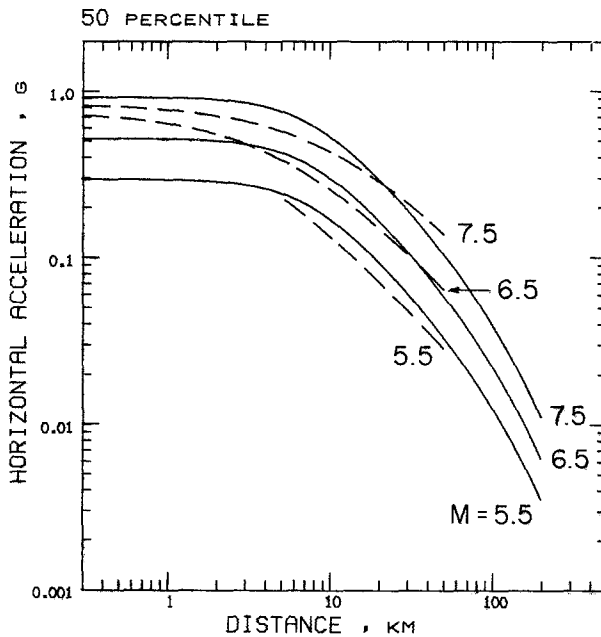


FIG. 13. Comparison of attenuation curves for peak horizontal acceleration by Campbell (1981) (dashed lines) with the 50 percentile curves from this report (solid lines). Campbell's curves are raised by 13 per cent to compensate for the fact that he defined peak horizontal acceleration as the mean of the two components rather than the larger one as we did.

to directivity. The effect of directivity would be to increase the peak velocity preferentially at sites near the fault. This effect would be reflected in a smaller value for h . Directivity would be expected to have a similar effect on peak acceleration (Boore and Joyner, 1978; Boore and Porcella, 1980), but one might speculate that local variations in the direction of rupture propagation or scattering and lateral refraction might in some way reduce the effect of directivity upon the higher frequency waves dominant in the acceleration record.

The magnitude coefficient in the relationship for peak acceleration is 0.25 and has a standard error of 0.04. It thus differs by little more than one standard error from the value 0.30, which corresponds to the scaling of peak acceleration as $M_0^{1/5}$ derived theoretically by Hanks and McGuire (1981) by treating the acceleration record as a stochastic process. The magnitude coefficient for peak velocity is 0.49 with a

standard error of 0.06. It lies within one standard error of the value 0.5, which corresponds to the scaling of peak velocity as $M_0^{1/3}$, appropriate for a deterministic rupture propagating outward from a point (Boatwright, 1980, oral communication, 1981; McGarr, 1981). It seems quite reasonable that the acceleration should look like a stochastic process and the velocity like a deterministic process.

ACKNOWLEDGMENTS

Unpublished strong-motion data were generously supplied to us by the California Division of Mines and Geology, by J. N. Brune on behalf of the University of California at San Diego and the Universidad Nacional Autonoma de Mexico, and by Kinometrics Inc. and the Shell Oil Co. We benefited significantly from discussion with T. C. Hanks. J. Boatwright and C. Rojahn critically reviewed the manuscript and made a number of valuable suggestions. We are indebted to K. W. Campbell for extended helpful discussions.

APPENDIX

The theoretical arguments for a magnitude-dependent shape, referred to in the text, are based on consideration of the scaling of peak acceleration with magnitude at close and far distances, and follow from an extension of the reasoning given in Hanks and McGuire (1981). Their stochastic source model predicts that the acceleration time history is to a good approximation a finite-duration sample of band-limited white, Gaussian noise. Using a result from Vanmarcke and Lai (1980), Hanks and McGuire (1981) give the following expression for the peak acceleration at a site whose distance to the source is large compared to the source dimensions

$$A_{\max} = A_{\text{rms}} \left(2 \ln \left[\frac{2S_0}{T_0} \right] \right)^{1/2} \quad (\text{A1})$$

where A_{rms} is the root-mean-square acceleration, S_0 is the duration of the acceleration time history, and T_0 is the predominant period of the acceleration.

By the Hanks and McGuire source theory, A_{rms} scales as $M_0^{1/6}$ and, given the moment-magnitude relation of equation (3), $\log A_{\text{rms}}$ is thereby proportional to moment magnitude with a coefficient of 0.25. Using their scaling of S_0 in terms of moment and assuming T_0 equals 0.2 sec, the logarithm of

$$\left(2 \ln \left[\frac{2S_0}{T_0} \right] \right)^{1/2}$$

is approximately proportional to moment magnitude in the range between 6.5 and 7.5 with a coefficient of 0.05. Combining the two factors gives a magnitude coefficient of 0.30 for $\log A_{\max}$. (As stated in the text, this compares with our value of 0.25, which has a standard deviation of 0.04. The difference is only slightly greater than the standard deviation.)

Further considerations are needed for the magnitude scaling close to the source. At small distance from a large source only a restricted portion of the source has an opportunity to generate the peak accelerations. In other words, the effective duration S_0 is fixed even as moment magnitude increases. Furthermore since the predominant period T_0 in Hanks and McGuire's analysis is independent of magnitude, the bracketed term in equation (A1) will also be magnitude independent. A_{\max} at small distance should then scale with magnitude in the same way as A_{rms} , provided that

A_{rms} is measured over the restricted portion of the record that corresponds to the effective duration. But A_{rms} measured over a fixed interval should scale with magnitude in the same way as A_{rms} over the whole record scales at distant stations. The difference in magnitude coefficient between near and distant stations is just the quantity

$$\log\left(2\ln\left[\frac{2S_0}{T_0}\right]\right)^{1/2}$$

which we have found to be 0.05 in the magnitude range 6.5 to 7.5. By choosing $h_2 = 0.12$ in our equations, we can force the 0.05 difference in magnitude coefficient between near and distant stations.

REFERENCES

- Aki, K. (1980). Scattering and attenuation of shear waves in the lithosphere, *J. Geophys. Res.* **85**, 6496-6504.
- Allen, C. R., T. C. Hanks, and J. H. Whitcomb (1973). San Fernando earthquake: seismological studies and their tectonic implications, in *San Fernando, California, Earthquake of February 9, 1971*, vol. 3, National Oceanic and Atmospheric Administration, U.S. Department of Commerce, 13-21.
- Ambraseys, N. N. (1974). Dynamics and response of foundation materials in epicentral regions of strong earthquakes, *Proc. World Conf. Earthquake Eng., 5th, Rome 1*, CXXVI-CXLVIII.
- Anderson, J. G. (1979). Estimating the seismicity from geological structure for seismic-risk studies, *Bull. Seism. Soc. Am.* **69**, 135-158.
- Boatwright, J. (1980). A spectral theory for circular seismic sources: simple estimates of source dimension, dynamic stress drop, and radiated seismic energy, *Bull. Seism. Soc. Am.* **70**, 1-27.
- Bolt, B. A. (1978). The local magnitude M_L of the Kern County earthquake of July 21, 1952, *Bull. Seism. Soc. Am.* **68**, 513-515.
- Bolt, B. A., T. V. McEvilly, and R. A. Uhrhammer (1981). The Livermore Valley, California, sequence of January 1980, *Bull. Seism. Soc. Am.* **71**, 451-463.
- Bolt, B. A. and R. D. Miller (1975). Catalogue of earthquakes in northern California and adjoining areas, 1 January 1910-31 December 1972, Seismographic Station, University of California, Berkeley, 567 pp.
- Boore, D. M. (1973). The effect of simple topography on seismic waves: implications for the accelerations recorded at Pacoima Dam, San Fernando Valley, California, *Bull. Seism. Soc. Am.* **63**, 1603-1609.
- Boore, D. M. and W. B. Joyner (1978). The influence of rupture incoherence on seismic directivity, *Bull. Seism. Soc. Am.* **68**, 283-300.
- Boore, D. M., W. B. Joyner, A. A. Oliver, III, and R. A. Page (1978). Estimation of ground motion parameters, *U.S. Geol. Surv., Circular 795*, 43 pp.
- Boore, D. M., W. B. Joyner, A. A. Oliver, III, and R. A. Page (1980). Peak acceleration, velocity, and displacement from strong-motion records, *Bull. Seism. Soc. Am.* **70**, 305-321.
- Boore, D. M. and R. L. Porcella (1980). Peak acceleration from strong-motion records: a postscript, *Bull. Seism. Soc. Am.* **70**, 2295-2297.
- Boore, D. M. and R. L. Porcella (1981). Peak horizontal ground motions from the 1979 Imperial Valley earthquake: comparison with data from previous earthquakes, in *The Imperial Valley, California Earthquake of October 15, 1979, U.S. Geol. Surv. Profess. Paper* (in press).
- Boore, D. M. and D. J. Stierman (1976). Source parameters of the Pt. Mugu, California, earthquake of February 21, 1973, *Bull. Seism. Soc. Am.* **66**, 385-404.
- Brady, A. G., P. N. Mork, V. Perez, and L. D. Porter (1980). Processed data from the Gilroy array and Coyote Creek records, Coyote Lake, California earthquake 6 August 1979, *U.S. Geol. Surv., Open-File Rept. 81-42*, 171 pp.
- Brune, J. N. (1968). Seismic moment, seismicity, and rate of slip along major fault zones, *J. Geophys. Res.* **73**, 777-784.
- Bufe, C. G., F. W. Lester, K. M. Lahr, J. C. Lahr, L. C. Seekins, and T. C. Hanks (1976). Oroville earthquakes: normal faulting in the Sierra Nevada foothills, *Science* **192**, 72-74.
- Campbell, K. W. (1981). Near-source attenuation of peak horizontal acceleration, *Bull. Seism. Soc. Am.* **71**, 2039-2070.

- Campbell, K. W., D. K. Davis, and F. W. Brady (1980). Attenuation of peak acceleration in the near-source region of earthquakes (abstract), *Trans. Am. Geophys. Union* **61**, 1035-1036.
- Cloud, W. K. (1959). Intensity and ground motion of the San Francisco earthquake of March 22, 1957, in *San Francisco Earthquakes of March, 1957, Calif. Div. Mines Special Report 57*, 49-57.
- Cloud, W. K. and J. F. Stifler (1976). Earthquakes and the registration of earthquakes from July 1, 1974 to December 31, 1974, *Bull. Seismographic Stations*, University of California, Berkeley, vol. 44, 86 pp.
- Cockerham, R. S., F. W. Lester, and W. L. Ellsworth (1980). A preliminary report on the Livermore Valley earthquake sequence January 24-February 26, 1980, *U.S. Geol. Surv., Open-File Rept. 80-714*, 45 pp.
- Crouse, C. B. (1978). Prediction of free-field earthquake ground motions, *Proc. ASCE Geotech. Eng. Div. Specialty Conf. Earthquake Eng. Soil Dynamics, Pasadena, Calif.* **1**, 359-379.
- Donovan, N. C. (1973). Earthquake hazards for buildings, in *Building Practice for Disaster Mitigation*, National Bureau of Standards Building Science Series **46**, 82-111.
- Draper, N. R. and H. Smith (1966). *Applied Regression Analysis*, Wiley, New York, 407 pp.
- Duke, C. M., K. E. Johnsen, L. E. Larson, and D. C. Engman (1972). Effects of site classification and distance on instrumental indices in the San Fernando earthquake, University of California, Los Angeles, School of Engineering and Applied Science, UCLA-ENG-7247, 29 pp.
- Dunbar, W. S., D. M. Boore, and W. Thatcher (1980). Pre-, co-, and postseismic strain changes associated with the 1952 $M_L = 7.2$ Kern County, California, earthquake, *Bull. Seism. Soc. Am.* **70**, 1893-1905.
- Ellsworth, W. L. (1975). Bear Valley, California, earthquake sequence of February-March 1972, *Bull. Seism. Soc. Am.* **65**, 483-506.
- Ellsworth, W. L., R. H. Campbell, D. P. Hill, R. A. Page, R. W. Alewine, III, T. C. Hanks, T. H. Heaton, J. A. Hileman, H. Kanamori, B. Minster, and J. H. Whitcomb (1973). Point Magu, California, earthquake of 21 February 1973 and its aftershocks, *Science* **182**, 1127-1129.
- Fogleman, K., R. Hansen, and R. Miller (1977). Earthquakes and the registration of earthquakes from July 1, 1975 to December 31, 1975, *Bull. Seismographic Stations*, University of California, Berkeley, vol. 45, 95 pp.
- Hamilton, R. M. (1972). Aftershocks of the Borrego Mountain earthquake from April 12 to June 12, 1968, in *The Borrego Mountain Earthquake of April 9, 1968, U.S. Geol. Surv. Profess. Paper 787*, 31-54.
- Hanks, T. C., J. A. Hileman, and W. Thatcher (1975). Seismic moments of the larger earthquakes of the southern California region. *Bull. Geol. Soc. Am.* **86**, 1131-1139.
- Hanks, T. C. and H. Kanamori (1979). A moment magnitude scale, *J. Geophys. Res.* **84**, 2348-2350.
- Hanks, T. C. and R. K. McGuire (1981). The character of high-frequency strong ground motion, *Bull. Seism. Soc. Am.* **71**, 2071-2095.
- Hanks, T. C. and M. Wyss (1972). The use of body-wave spectra in the determination of seismic-source parameters, *Bull. Seism. Soc. Am.* **62**, 561-568.
- Hart, R. S., R. Butler, and H. Kanamori (1977). Surface-wave constraints on the August 1, 1975, Oroville earthquake, *Bull. Seism. Soc. Am.* **67**, 1-7.
- Hasegawa, H. S., J. C. Lahr, and C. D. Stephens (1980). Fault parameters of the St. Elias, Alaska, earthquake of February 28, 1979, *Bull. Seism. Soc. Am.* **70**, 1651-1660.
- Heaton, T. H. and D. V. Helmberger (1979). Generalized ray models of the San Fernando earthquake, *Bull. Seism. Soc. Am.* **69**, 1311-1341.
- Herd, D. G., W. L. Ellsworth, A. G. Lindh, and K. M. Shedlock (1981). Future large earthquakes in the San Francisco Bay area (submitted for publication).
- Jennings, P. C. and H. Kanamori (1979). Determination of local magnitude, M_L , from seismoscope records, *Bull. Seism. Soc. Am.* **69**, 1267-1288.
- Johnson, L. R. and T. V. McEvelly (1974). Near-field observations and source parameters of central California earthquakes, *Bull. Seism. Soc. Am.* **64**, 1855-1886.
- Joyner, W. B., D. M. Boore, and R. L. Porcella (1981). Peak horizontal acceleration and velocity from strong-motion records (abstract), *Earthquake Notes* **52**, 80-81.
- Kanamori, H. (1978). Semi-empirical approach to prediction of ground motions produced by large earthquakes, *Proc. NSF Seminar Workshop on Strong Ground Motion*, California Institute of Technology, Pasadena, 80-84.
- Kanamori, H. and P. C. Jennings (1978). Determination of local magnitude, M_L , from strong-motion accelerograms, *Bull. Seism. Soc. Am.* **68**, 471-485.
- Knudson, C. F. and F. Hansen A. (1973). Accelerograph and seismoscope records from Managua, Nicaragua earthquakes, in *Managua, Nicaragua Earthquake of December 23, 1972, Proc. Earthquake Eng. Research Inst. Conf.* **1**, 180-205.

- Lahr, K. M., J. C. Lahr, A. G. Lindh, C. G. Bufe, and F. W. Lester (1976). The August 1975 Oroville earthquakes, *Bull. Seism. Soc. Am.* **66**, 1085-1099.
- Langston, C. A. and R. Butler (1976). Focal mechanism of the August 1, 1975 Oroville earthquake, *Bull. Seism. Soc. Am.* **66**, 1111-1120.
- Lee, W. H. K., D. G. Herd, V. Cagnetti, W. H. Bakun, and A. Rapport (1979). A preliminary study of the Coyote Lake earthquake of August 6, 1979 and its major aftershocks, *U.S. Geol. Surv., Open-File Rept. 79-1621*, 43 pp.
- Lee, W. H. K., C. E. Johnson, T. L. Henyey, and R. L. Yerkes (1978). A preliminary study of the Santa Barbara, California, earthquake of August 13, 1978, and its major aftershocks, *U.S. Geol. Surv. Circular 797*, 11 pp.
- Lindh, A. G. and D. M. Boore (1981). Control of rupture by fault geometry during the 1966 Parkfield earthquake, *Bull. Seism. Soc. Am.* **71**, 95-116.
- McEvelly, T. V., W. H. Bakun, and K. B. Casaday (1967). The Parkfield, California, earthquakes of 1966, *Bull. Seism. Soc. Am.* **57**, 1221-1244.
- McGarr, A. (1981). Analysis of peak ground motion in terms of a model of inhomogeneous faulting, *J. Geophys. Res.* **86**, 3901-3912.
- McGuire, R. K. (1978). Seismic ground motion parameter relations, *Proc. Am. Soc. Civil Eng. J. Geotech. Eng. Div.* **104**, 481-490.
- Molnar, P. (1979). Earthquake recurrence intervals and plate tectonics, *Bull. Seism. Soc. Am.* **69**, 115-133.
- Page, R. A., D. M. Boore, W. B. Joyner, and H. W. Coulter (1972). Ground motion values for use in the seismic design of the trans-Alaska pipeline system, *U.S. Geol. Surv. Circular 672*, 23 pp.
- Page, R. A. and W. H. Gawthrop (1973). The Sitka, Alaska, earthquake of 30 July 1972 and its aftershocks (abstract), *Earthquake Notes* **44**, 16-17.
- Plafker, G. and R. D. Brown, Jr. (1973). Surface geologic effects of the Managua earthquake of December 23, 1972, in *Managua, Nicaragua Earthquake of December 23, 1972, Proc. Earthquake Eng. Research Inst. Conf. 1*, 115-142.
- Porcella, R. L. (Editor) (1979). Seismic Engineering Program Report, *U.S. Geol. Surv. Circular 818-A*, 20 pp.
- Porcella, R. L., R. B. Matthiesen, R. D. McJunkin, and J. T. Ragsdale (1979). Compilation of strong-motion records from the August 6, 1979 Coyote Lake earthquake, *U.S. Geol. Surv., Open-File Rept. 79-385*, 71 pp.
- Porter, L. D. (1978). Compilation of strong-motion records recovered from the Santa Barbara earthquake of 13 August 1978, *Calif. Div. Mines and Geol. Prelim. Rept. 22*, 43 pp.
- Purcaru, G. and H. Berckhemer (1978). A magnitude scale for very large earthquakes, *Tectonophysics* **49**, 189-198.
- Richter, C. F. (1935). An instrumental earthquake magnitude scale, *Bull. Seism. Soc. Am.* **25**, 1-32.
- Richter, C. F. (1958). *Elementary Seismology*, W. H. Freeman, San Francisco, 768 pp.
- Scholz, C. H. (1981). Scaling laws for large earthquakes: consequences for physical models (submitted for publication).
- Shannon and Wilson, Inc. and Agbajian Associates (1978). Verification of subsurface conditions at selected "rock" accelerograph stations in California Volume 1, U.S. Nuclear Regulatory Commission NUREG/CR-0055, Clearinghouse, Springfield, Virginia 22151.
- Shannon and Wilson, Inc. and Agbajian Associates (1980a). Verification of subsurface conditions at selected "rock" accelerograph stations in California Volume 2, U.S. Nuclear Regulatory Commission NUREG/CR-0055, Clearinghouse, Springfield, Virginia 22151.
- Shannon and Wilson, Inc. and Agbajian Associates (1980b). Geotechnical data from accelerograph stations investigated during the period 1975-1979, U.S. Nuclear Regulatory Commission NUREG/CR-1643, Clearinghouse, Springfield, Virginia, 22151.
- Stierman, D. J. and W. L. Ellsworth (1976). Aftershocks of the February 21, 1973 Point Mugu, California earthquake, *Bull. Seism. Soc. Am.* **66**, 1931-1952.
- Swanger, H. J. and D. M. Boore (1978). Simulation of strong-motion displacements using surface-wave modal superposition, *Bull. Seism. Soc. Am.* **68**, 907-922.
- Tocher, D. (1959). Seismographic results from the 1957 San Francisco earthquakes, in *San Francisco Earthquakes of March 1957, Calif. Div. Mines Special Rept. 57*, 59-71.
- Trifunac, M. D. (1972). Tectonic stress and the source mechanism of the Imperial Valley, California, earthquake of 1940, *Bull. Seism. Soc. Am.* **62**, 1283-1302.
- Trifunac, M. D. (1976). Preliminary analysis of the peaks of strong earthquake ground motion—Dependence of peaks on earthquake magnitude, epicentral distance, and recording site conditions,

- Bull. Seism. Soc. Am.* **66**, 189-219.
- Trifunac, M. D. and J. N. Brune (1970). Complexity of energy release during that Imperial Valley, California, earthquake of 1940, *Bull. Seism. Soc. Am.* **60**, 137-160.
- Trifunac, M. D. and F. E. Udawadia (1974). Parkfield, California, earthquake of June 27, 1966: a three-dimensional moving dislocation, *Bull. Seism. Soc. Am.* **64**, 511-533.
- Tsai, Y.-B. and K. Aki (1969). Simultaneous determination of the seismic moment and attenuation of seismic surface waves, *Bull. Seism. Soc. Am.* **59**, 275-287.
- Uhrhammer, R. A. (1980). Observations of the Coyote Lake, California earthquake sequence of August 6, 1979, *Bull. Seism. Soc. Am.* **70**, 559-570.
- Unger, J. D. and J. P. Eaton (1970). Aftershocks of the October 1, 1969, Santa Rosa, California, earthquakes (abstract), *Geol. Soc. Am. Abstracts with Programs* **2**, 155.
- U.S. Dept. of Commerce (1973). Earthquake Data Report EDR No. 76-72.
- U.S. Geological Survey (1977). Western hemisphere strong-motion accelerograph station list—1976, *U.S. Geol. Surv., Open-File Rept. 77-374*, 112 pp.
- Vanmarcke, E. H. and S.-S. P. Lai (1980). Strong-motion duration and rms amplitude of earthquake records, *Bull. Seism. Soc. Am.* **70**, 1293-1307.
- Wallace, T. C. and D. V. Helmberger (1979). A model of the strong ground motion of the August 13, 1978 Santa Barbara earthquake (abstract), *EOS Trans. Am. Geophys. Union* **60**, 895.
- Ward, P. L., D. Harlow, J. Gibbs, and A. Aburto Q. (1973). Location of the main fault that slipped during the Managua earthquake as determined from locations of some aftershocks, in *Managua, Nicaragua Earthquake of December 23, 1972, Proc. Earthquake Eng. Research Inst. Conf.* **1**, 89-96.
- Weisberg, S. (1980). *Applied Linear Regression*, Wiley, New York, 283 pp.